

**Structural investigation of GeSb<sub>2</sub>Te<sub>4</sub>: A high-speed phase-change material**Toshiyuki Matsunaga<sup>1,\*</sup> and Noboru Yamada<sup>2</sup><sup>1</sup>Characterization Technology Group, Matsushita Technoresearch, Inc., Osaka 570-8501, Japan<sup>2</sup>Storage Media Systems Development Center, Matsushita Electric Industrial Co., Ltd., 3-1-1 Yagumo-Nakamachi, Moriguchi, Osaka 570-8501, Japan

(Received 21 March 2003; published 26 March 2004)

Pseudobinary GeTe-Sb<sub>2</sub>Te<sub>3</sub> is in wide use today as a memory material in phase-change optical disks such as DVD-RAMs. GeSb<sub>2</sub>Te<sub>4</sub>, one of the intermetallic compounds used in this binary system, when in thermal equilibrium, shows a complex cubic close-packed structure with a 21-layer period. However, when an amorphous thin film of this compound is heated by laser irradiation and then suddenly cooled, it crystallizes into a simple NaCl-type structure as the metastable phase. These two structures are so different from each other that it is difficult to imagine that they have the same chemical composition. To reveal the relationship between the two, in this paper we examine the structures of both phases of GeSb<sub>2</sub>Te<sub>4</sub> at various temperatures by x-ray powder diffraction using synchrotron radiation facilities. The results of our investigation are as follows: the metastable phase has a very open structure, which contains one vacancy per eight atoms. The structure transition from the metastable to the stable phase is due to the vacancy diffusion. Contrary to what was previously thought, the crystal structure of the stable phase is similar to that of PbBi<sub>2</sub>Se<sub>4</sub>.

DOI: 10.1103/PhysRevB.69.104111

PACS number(s): 61.10.-i, 64.60.-i

**I. INTRODUCTION**

In a rewritable optical disk such as a DVD-RAM, information is recorded using the difference in optical characteristics caused by the phase change in the material. The best known phase-change material at present is GeTe-Sb<sub>2</sub>Te<sub>3</sub> a pseudobinary compound. In this compound, a reversible structural change between the crystal and amorphous phases is induced by a very brief laser irradiation lasting several tens of nanoseconds; this alters the optical characteristics of the recording layer in the disk such as the reflectivity or transmissivity. During recording, the area to be recorded is heated to above the melting point (around 900 K) using a high-power laser beam; it then instantaneously cools, forming an amorphous mark. On the other hand, when erasing, the mark is annealed up to around 700 K by using a middle-power laser beam, which causes recrystallization. To play back the recorded signal, a low-power laser beam, which does not affect the recording marks, is used to detect and read the difference in reflectivity between the amorphous and crystal phases.

It is known that the GeTe-Sb<sub>2</sub>Te<sub>3</sub> pseudobinary system, when in thermal equilibrium, forms three intermetallic compounds: Ge<sub>2</sub>Sb<sub>2</sub>Te<sub>5</sub>, GeSb<sub>2</sub>Te<sub>4</sub>, and GeSb<sub>4</sub>Te<sub>7</sub>.<sup>1</sup> These three compounds are described as cubic close-packed structures in which the Ge, Sb, and Te layers are stacked in different periods. Ge<sub>2</sub>Sb<sub>2</sub>Te<sub>5</sub>, GeSb<sub>2</sub>Te<sub>4</sub>, and GeSb<sub>4</sub>Te<sub>7</sub> are nine-layer ( $P\bar{3}m1, 4.20 \times 16.96 \text{ \AA}$ ), 21-layer ( $R\bar{3}m, 4.21 \times 40.6 \text{ \AA}$ ), and 12-layer ( $P\bar{3}m1, 4.21 \times 23.65 \text{ \AA}$ ) structures, respectively.<sup>2,3</sup> GeTe and Sb<sub>2</sub>Te<sub>3</sub> are described as six-layer<sup>4</sup> and 15-layer<sup>5</sup> structures, respectively. The GeTe-Sb<sub>2</sub>Te<sub>3</sub> pseudobinary compound, however, crystallizes into a single metastable phase with a NaCl-type structure ( $Fm\bar{3}m$ ) after heating and instantaneous cooling (erasing) by laser irradiation over a wide range from 100 mol% to at least 50 mol% of GeTe. In this structure, the 4(*a*) site is fully occupied by Te atoms, whereas the 4(*b*) site is

randomly occupied by Ge and Sb atoms and vacancies. When the composition of this binary system is described as (GeTe)<sub>x</sub> + (Sb<sub>2</sub>Te<sub>3</sub>)<sub>1-x</sub>; ( $0 \leq x \leq 1$ ), the site occupancy of the vacancy varies continuously according to  $(1-x)/(3-2x)$ .<sup>6</sup>

The authors have, in recent years, carried out precise examinations, using synchrotron radiation, of the crystal structures of Au-Ge-Sn-Te (Ref. 7) and Ag-In-Sb-Te quadruple compounds,<sup>8</sup> which are used for CD-RWs, etc., as well as the GeTe-Sb<sub>2</sub>Te<sub>3</sub> pseudobinary compound,<sup>9</sup> and on the relationship between their structures and temperature. A large-diameter Debye-Scherrer camera<sup>10</sup> installed in the BL02B2 beam line at SPring-8 can obtain diffraction patterns with a much higher angular resolution than conventional x-ray diffractometers used in laboratories. Using this camera, we succeeded in revealing for the first time, to our knowledge, the

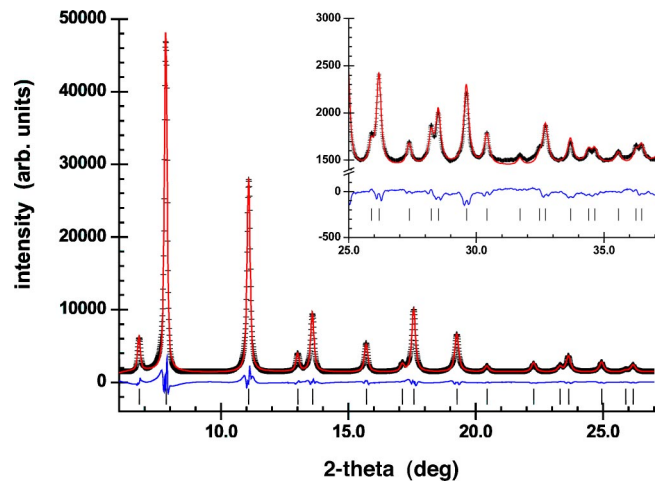


FIG. 1. (Color online) Observed (+) and calculated (gray line) x-ray diffraction profiles of GeSb<sub>2</sub>Te<sub>4</sub> metastable phase at room temperature (300 K). A difference curve (observed-calculated) appears at the bottom of each figure, and, under the curve, the reflection markers are indicated by the vertical rods.

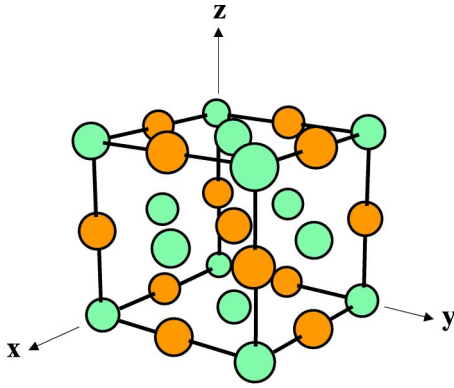


FIG. 2. (Color online) Crystal structure of laser-crystallized metastable  $\text{GeSb}_2\text{Te}_4$  shown schematically in perspective. Black filled circles show atomic positions for Te. Gray-painted circles show those for Ge or Sb.

crystal structure of the Ag-In-Sb-Te compound. Synchrotron radiation facilities generate intense x rays, making it possible to collect precise x-ray diffraction data within a reasonably short time. This method is useful for high temperature measurements on materials containing elements that oxidize easily, such as Sb and Te.

Of the intermetallic compounds with stable phases seen in the GeTe-Sb<sub>2</sub>Te<sub>3</sub> pseudobinary system,  $\text{GeSb}_2\text{Te}_4$  has the most complex structure. On the other hand, its metastable phase crystallizes into a NaCl-type simple structure. In this study, each crystal structure of these two phases was analyzed in detail, and the dependence of the crystal structure on temperature was examined in detail to reveal the structure transition mechanism from the metastable to the stable phase.

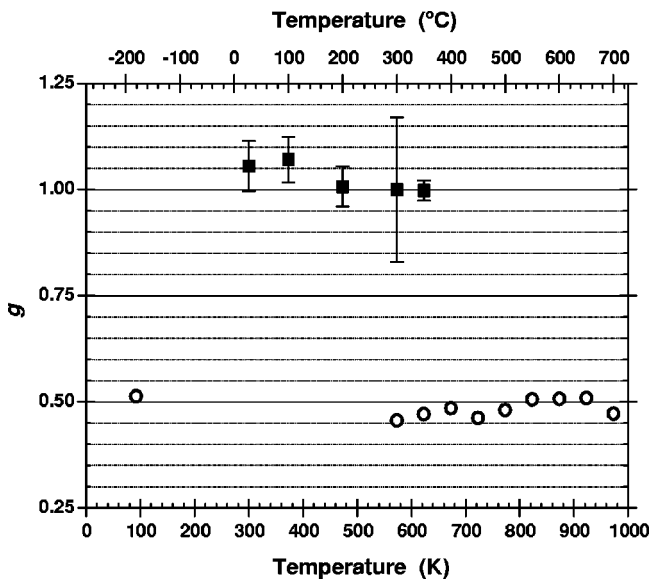


FIG. 3. Temperature dependence of the  $g$  parameter at the  $4(b)$  site of the metastable phase and at the  $3(a)$  site of the stable phase. Black filled squares and open circles show the metastable and stable phases, respectively. The errors estimated about the latter are smaller than the marks.

TABLE I. Refined structural parameters for the  $\text{GeSb}_2\text{Te}_4$  metastable phase at room temperature. Standard deviations are shown in parentheses. The final  $R$  factors and lattice parameter are  $R_{\text{wp}} = 6.01\%$ ,  $R_p = 3.83\%$ ,  $R_I = 1.79\%$ ,  $R_{\text{wp expected}} = 2.10\%$ , and  $a = 6.0430(9)$  Å.

Atom	Site	$x$	$y$	$z$	$B$ (Å <sup>2</sup> )
Te <sub>1.0</sub>	4( $a$ )	0	0	0	1.4(3)
Ge <sub>0.25</sub> Sb <sub>0.50</sub>	4( $b$ )	1/2	1/2	1/2	3.2(5)

Our results show that the layer stacking of Ge, Sb, and Te in the crystal structure of the stable phase is different from that previously reported; and, in addition, Ge and Sb atoms simultaneously occupy two sites rather than locate individually at their respective sites. The atomic positions and site occupancies change very little in either the stable or metastable phase except for simple thermal expansion of the lattice, irrespective of temperature. We believe this phase transition not to be due to the shifts in atomic position or changes in site occupancy usually seen in various phase transition materials, but to arise from the annihilation of the specific Ge/Sb layers caused by vacancy diffusion.

## II. EXPERIMENT

The specimen for diffraction measurement was made using the following method. First, a thin film of  $\text{GeSb}_2\text{Te}_4$  with a thickness of approximately 5000 Å was formed by sputtering on a glass disk with a diameter of 120 mm. The film is amorphous just after its formation. The film was crystallized into the metastable crystal phase by means of laser irradiation and was then scraped off with a spatula to create a

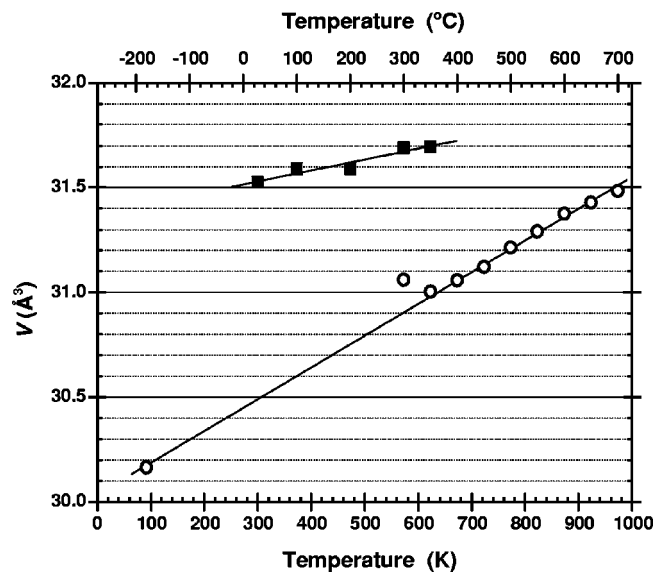


FIG. 4. Temperature dependence of the mean volume per single atom. Black filled squares and open circles show the metastable and the stable phases, respectively. The estimated errors are smaller than the marks. Two lines in the figure were obtained by the least squares method for each phase.

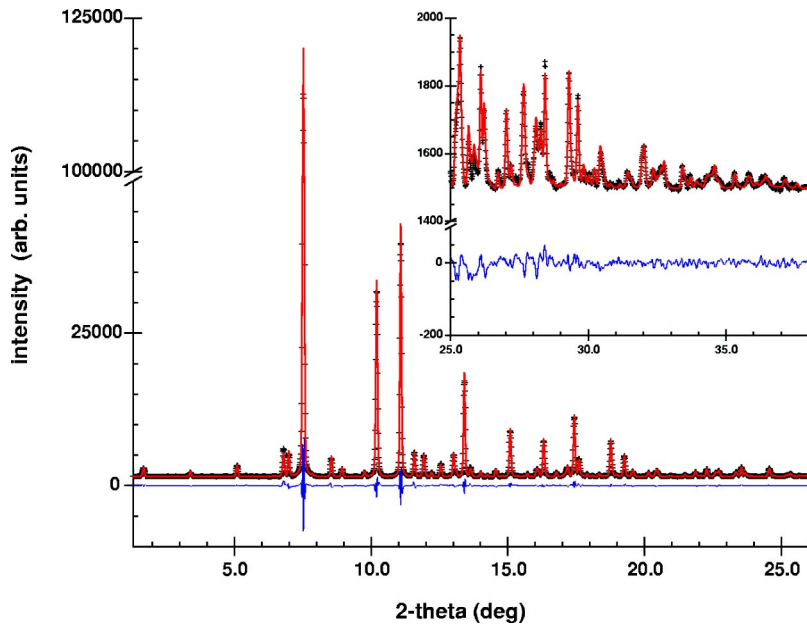


FIG. 5. (Color online) Observed (+) and calculated (gray line) x-ray diffraction profiles of the  $\text{GeSb}_2\text{Te}_4$  stable phase at a temperature of 873 K. A difference curve (observed-calculated) appears at the bottom of each figure.

powder. The specimens for diffraction experiments using the synchrotron radiation were made by packing the powder into quartz capillary tubes with an external diameter of 0.2 mm. To insulate the specimen from the atmosphere, the capillaries were sealed at both ends by melting with an oxyacetylene flame.

The diffraction experiments were carried out using the large-diameter Debye-Scherrer camera with an imaging plate on the BL02B2 beam line at the Japan Synchrotron Radiation Research Institute (SPring-8). A pre-collimator mirror

and a double crystal monochromator were used to ensure that the incident beam used for the diffraction experiments was extremely monochromatic and parallel. The camera radius was 278 mm and the pixel area of the imaging plate was  $100 \mu\text{m}^2$ , corresponding to an angular resolution of  $0.02^\circ$ . The crystal structure was precisely determined using the Rietveld method.<sup>11</sup> The program used was RIETAN.<sup>12</sup> To improve the accuracy of the Rietveld analysis, intensity data in steps of  $0.01^\circ$  were obtained by reading the imaging plate at a pixel area of  $50 \mu\text{m}^2$ .

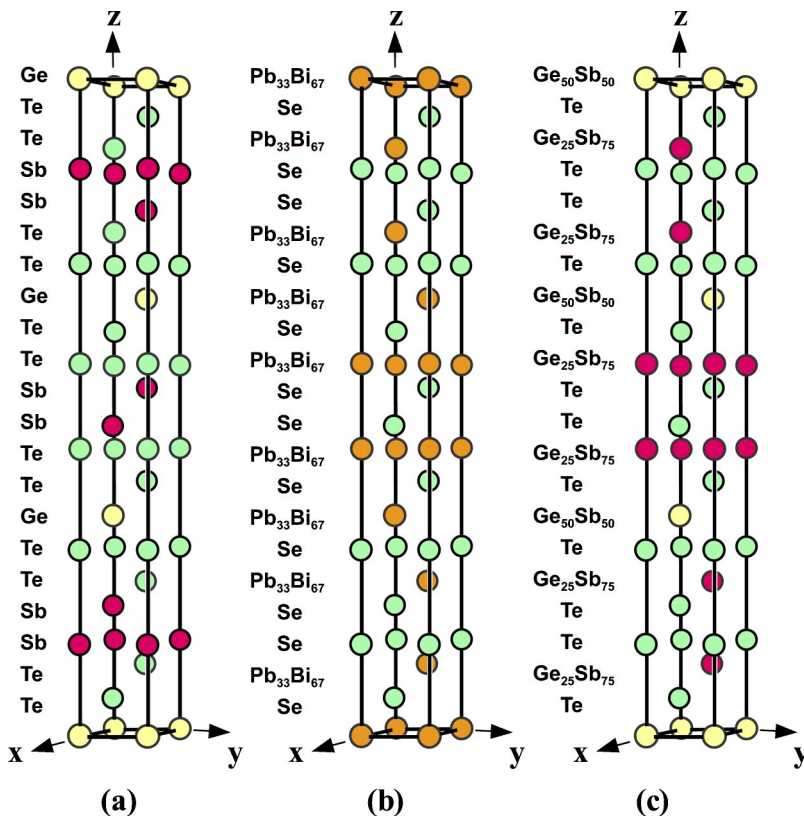


FIG. 6. (Color online) The crystal structures of (a) the  $\text{GeSb}_2\text{Te}_4$  stable phase analyzed by Agaev *et al.*, (b)  $\text{PbBi}_2\text{Se}_4$ , and (c) derived by our investigation, shown schematically in perspective.

TABLE II. Structural parameters for (a)  $\text{GeSb}_2\text{Te}_4$  shown by Agaev and Talybov (Ref. 3), (b)  $\text{GeBi}_2\text{Te}_4$ , and (c)  $\text{PbBi}_2\text{Se}_4$  shown by Agaev and Semiletov (Refs. 15 and 16). The space group is  $R\bar{3}m$  (Ref. 13), (a)  $a=4.21 \text{ \AA}$ ,  $c=40.6 \text{ \AA}$ , (b)  $a=4.28 \text{ \AA}$ ,  $c=39.2 \text{ \AA}$ , and (c)  $a=4.16 \text{ \AA}$ ,  $c=39.2 \text{ \AA}$ .  $\text{PbBi}_2\text{Se}_4$  has the same Pb/Bi ratio at the 3(a) and 6(c) sites.

(a) Atom	Site	$x$	$y$	$z$
Ge	3(a)	0	0	0
Sb	6(c)	0	0	0.144
Te(1)	6(c)	0	0	0.290
Te(2)	6(c)	0	0	0.432
(b) Atom	Site	$x$	$y$	$z$
Ge	3(a)	0	0	0
Te(1)	6(c)	0	0	0.136
Te(2)	6(c)	0	0	0.289
Bi	6(c)	0	0	0.425
(c) Atom	Site	$x$	$y$	$z$
(Pb, 2Bi)	3(a)	0	0	0
Se(1)	6(c)	0	0	0.139
Se(2)	6(c)	0	0	0.286
(Pb, 2Bi)	6(c)	0	0	0.428

The energy of the incident x-ray beam was 30.039 keV ( $\lambda=0.4127 \text{ \AA}$ ), which was confirmed by recording the diffraction pattern of a  $\text{CeO}_2$  standard powder specimen ( $a=5.4111 \text{ \AA}$ ) at room temperature under the same conditions as the reference sample. The experiments at low and high temperatures were conducted while blowing  $\text{N}_2$  gas at a predetermined temperature over the capillary. Temperature calibration was carried out by using a thermocouple placed at the specimen position. This established the accuracy of the temperature within  $\pm 10 \text{ K}$  over a range of 90–1000 K. Inductively coupled plasma atomic emission spectrometry confirmed that the composition of the specimen was close to  $\text{GeSb}_2\text{Te}_4$ .

### III. RESULTS

The  $\text{GeSb}_2\text{Te}_4$  film was amorphous just after formation and was then crystallized in advance into a metastable NaCl-type structure by laser irradiation. When this metastable phase is heated, structural transition to the stable phase be-

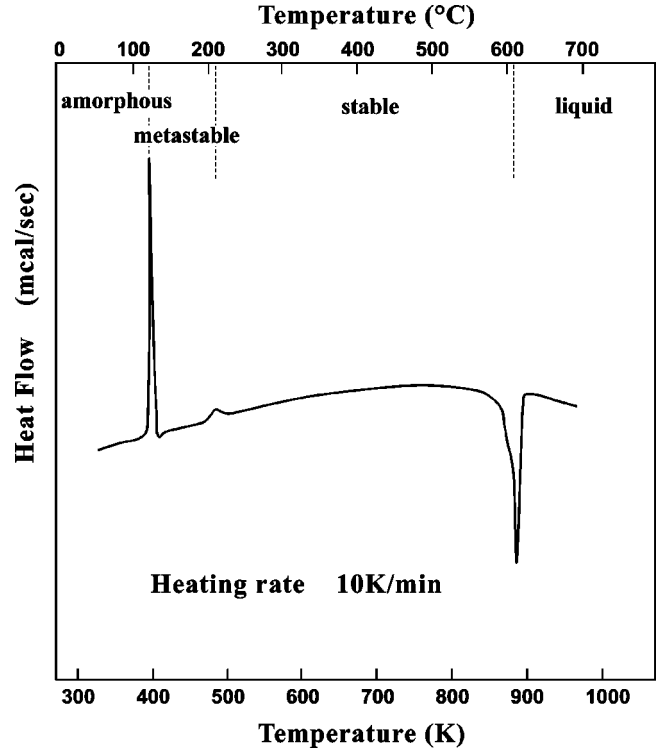


FIG. 7. DSC curve when heating an amorphous  $\text{GeSb}_2\text{Te}_4$  powdered specimen measured by Yamada *et al.* (Ref. 17).

gins at around 500 K. Once the structure had changed, the stable phase maintained a uniform structure up to around the melting point. In addition, the structure remained unchanged when the temperature was subsequently reduced to 90 K. The crystal structure and its relation to temperature revealed by the synchrotron radiation experiments are described below.

#### A. Crystal structure of the metastable phase

The results of our structure analysis of the metastable phase are shown in Table I and Fig. 1. This phase belongs to the space group  $Fm\bar{3}m$ .<sup>13</sup> Of the three elements, Te atoms occupied 100% of the 4(a) site, and Ge and Sb occupied the 4(b) site at random, showing a NaCl-type structure (Fig. 2). The 4(b) sites were not completely filled with atoms, and contained about 25-at. % vacancies. To confirm that the 4(b) site definitely contained such a large number of vacancies, that is, whether Te atoms invaded the 4(b) site,<sup>9</sup> we carried out the Rietveld analysis under the condition where the  $g$

TABLE III. Refined structural parameters for the  $\text{GeSb}_2\text{Te}_4$  stable structure at 873 K. The space group is  $R\bar{3}m$ . Standard deviations are shown in parentheses. The final  $R$  factors and lattice parameters are  $R_{\text{wp}}=3.93\%$ ,  $R_p=2.53\%$ ,  $R_I=1.22\%$ ,  $R_{\text{wp}} \text{ expected}=2.12\%$  and  $a=4.2721(3) \text{ \AA}$ ,  $c=41.686(2) \text{ \AA}$ .

Atom	Site	$g$	$x$	$y$	$z$	$B (\text{\AA}^2)$
Ge/Sb	3(a)	0.493/0.507(8)	0	0	0	4.08(9)
Te(1)	6(c)	1.0	0	0	0.13281(3)	3.40(6)
Te(2)	6(c)	1.0	0	0	0.29005(4)	2.94(4)
Ge/Sb	6(c)	0.253/0.747	0	0	0.42700(4)	5.23(8)

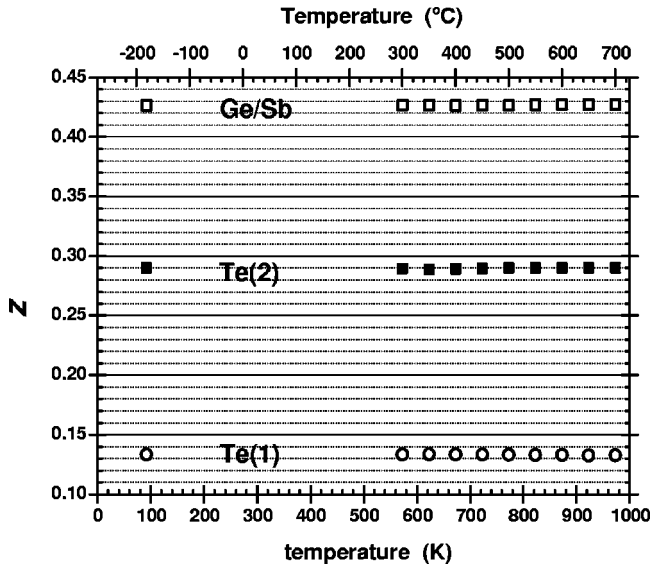


FIG. 8. Temperature dependence of the atomic position of  $z$  for Te(1), Te(2), and Ge/Sb at each 6(c) site.

parameter of the 4(b) site, which indicates the site occupancy of Ge<sub>0.25</sub>Sb<sub>0.5</sub>, was variable, and concluded that the value of  $g$  was unity within its standard deviation. Even with changes in temperature, this value remained almost constant at unity (Fig. 3). This result indicates that the metastable phase has only seven atoms per unit cell, rather than eight, regardless of temperature. The temperature dependence of the mean volume per single atom is shown in Fig. 4. From this figure it can be seen that the coefficient of volume expansion at room temperature of the metastable phase is  $1.65 \times 10^{-5}/\text{K}$ . We can see an obvious broadening of the peaks in Fig. 1. This suggests that, immediately after sputtering, the film consists of comparatively small crystallites and shows a large strain. The Wilson plot,<sup>14</sup> which was performed using all of the reflections in the figure, shows that the mean crystallite size and random strain were about 190 Å and 0.23%, respectively.

### B. Crystal structure of the stable phase

The diffraction peaks obtained at 873 K (Fig. 5) became considerably sharp compared with those of the metastable phase at 300 K. This is assumed to be due to the crystal growth and strain relief during the high-temperature measurements. The mean crystallite size and random strain were about 300 Å and 0.07%, respectively.

Agaev *et al.* analyzed the crystal structure of the GeSb<sub>2</sub>Te<sub>4</sub> stable phase. To our knowledge, we are the first to attempt a Rietveld analysis according to their structure model [Table II(a) and Fig. 6(a)] using the diffraction intensity data obtained at 873 K. The result, however, was not satisfactory ( $R_I=5.35\%$ ). It is known that, while GeBi<sub>2</sub>Te<sub>4</sub> (Ref. 15) has a 21-layer cubic close-packed structure like GeSb<sub>2</sub>Te<sub>4</sub> shown by Agaev *et al.*, the site occupation of the three elements is different from each other [compare (a) with (b) in Table II]. Next, adopting this structure as an initial model, we performed an analysis to obtain a better result

than the former ( $R_I=2.81\%$ ). However, especially with weaker diffraction peaks, a difference between the measured ( $I_o$ ) and calculated ( $I_c$ ) intensities still remained. We then carried out further analysis under the assumption that Ge (Pb) and Sb (Bi) occupy the 3(a) and 6(c) sites at random, as in PbBi<sub>2</sub>Se<sub>4</sub> (Ref. 16) [Table II(c) and Fig. 6(b)], and obtained an even better result ( $R_I=1.34\%$ ). According to this model, the Ge/Sb ratio should be equal at both sites. The layer stacking is, however, expressed as

$$\cdots \frac{\text{Ge/Sb}}{3(a)} \cdot \text{Te} \cdot \frac{\text{Ge/Sb}}{6(c)} \cdot \text{Te} \cdot \text{Te} \cdot \frac{\text{Ge/Sb}}{6(c)} \cdot \text{Te} \cdots$$

As noticed from this expression, the Ge/Sb layers at the 3(a) and 6(c) sites are sandwiched by the different stacking structures of the upper and lower layers, which affects the Ge/Sb ratio. To confirm the occupation rates of these two atoms at both sites, we set the following conditions for the Rietveld analysis:

$$g_{\text{Ge}}^{3(a)} = 1 - g_{\text{Sb}}^{3(a)}, \quad g_{\text{Ge}}^{6(c)} = g_{\text{Sb}}^{3(a)}/2 \quad \text{and} \quad g_{\text{Sb}}^{6(c)} = 1 - g_{\text{Sb}}^{3(a)}/2, \quad (1)$$

and resumed our analysis, taking  $g_{\text{Sb}}^{3(a)}$  as an independent variable. Here,  $g_{\text{Sb}}^{3(a)}$  represents the occupation rate of Sb at the 3(a) site. As shown in Table III and Fig. 5, this assumption showed a more satisfactory result. Although there remained some variance attributable to temperature changes, the value of  $g_{\text{Sb}}^{3(a)}$  was close to 0.5 (Fig. 3). It is consequently understood that the 3(a) and 6(c) sites are occupied approximately in the ratios of Ge:Sb=1:1 and 1:3 regardless of temperature. The determined crystal structure of GeSb<sub>2</sub>Te<sub>4</sub> is shown in Fig. 6(c).

As seen in Table III, the thermal vibrations of the Ge/Sb atoms at the 3(a) and 6(c) sites are greater than those of the Te atoms and are different from each other. We attribute these findings to the Ge atom being lighter than the other elements as well as to the difference in potential (binding) energy at both sites. The temperature dependence of the mean volume per single atom indicates the coefficient of volume expansion for the stable phase to be  $5.02 \times 10^{-5}/\text{K}$  at room temperature (see Fig. 4). Our measurements showed that the stable phase was maintained up to 973 K. Differential scanning calorimetry (DSC) measurements on amorphous GeSb<sub>2</sub>Te<sub>4</sub> have already been conducted by Yamada, one of the authors, *et al.*<sup>17</sup> (Fig. 7). The temperature of the DSC was calibrated by using a series of ICTA/NBS (International Confederation for Thermal Analysis/National Bureau of Standards) Standard Reference Materials<sup>18</sup> to achieve an accuracy within  $\pm 10$  K at a heating rate of 10 K/min over a range of 300–1000 K. The temperature of 973 K is higher than the melting point, at around 890 K, obtained by DSC measurement or as seen in the phase diagram shown by Abrikosov *et al.*<sup>1</sup> This difference is attributed to the pressure rise in the sealed capillary caused by the increase in temperature.

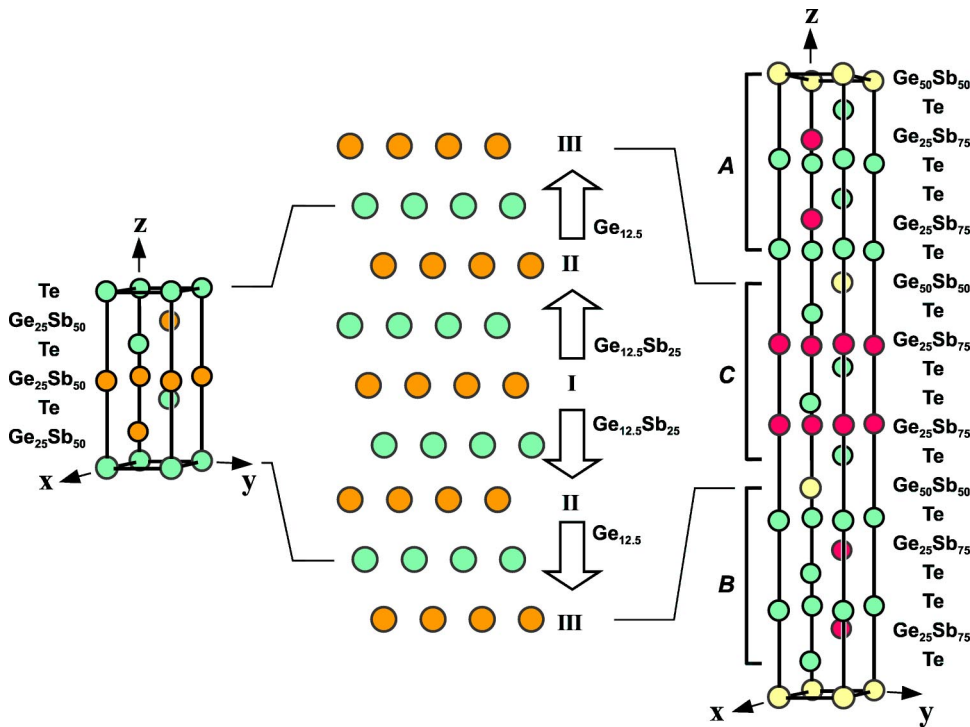


FIG. 9. (Color online) Schematic drawing of atomic diffusion in a metastable  $\text{GeSb}_2\text{Te}_4$  crystal. This diffusion causes the structural transition from the metastable phase (left) to the stable phase (right).

IV. DISCUSSION

A. Metastable phase

Since the metastable phase belongs to the  $Fm\bar{3}m$  space group in which atoms occupy  $4(a)$ ,  $0, 0, 0$ , and  $4(b)$ ,  $\frac{1}{2}, \frac{1}{2}, \frac{1}{2}$ , the relative atomic position remains constant even if the temperature changes. The number of vacancies in the  $4(b)$  site also altered only slightly (Fig. 3). The only observed change was thermal expansion of the lattice (Fig. 4). This metastable phase, however, suddenly transforms into a stable phase at

around 500 K. Figure 7 shows an exothermic peak at this transition point, which means that this structure transformation requires an activation energy.

B. Stable phase

The stable phase of  $\text{GeSb}_2\text{Te}_4$  has a 21-layer cubic close-packed structure, in which each layer is shifted by one-third of  $\bar{\mathbf{a}}_H + \mathbf{b}_H$ . According to Agaev *et al.*, the layer stacking takes the following form:

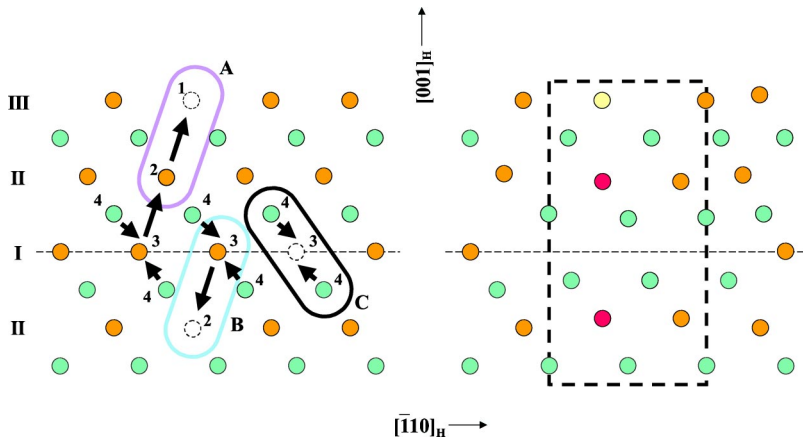
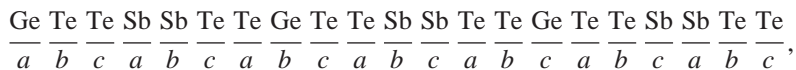
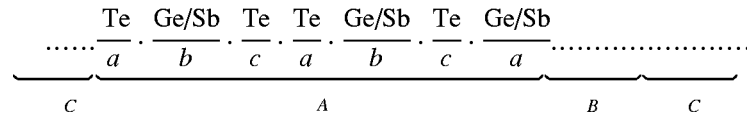


FIG. 10. (Color online) Structural phase transition caused by vacancy diffusion. The three types of atomic displacements shown in the drawing on the left form the atomic arrangement of the stable phase in the area surrounded by the dashed line in the drawing on the right.

with Ge and Sb occupying 100% of 3(*a*) and 6(*c*), respectively. In our analysis, however, the layer stacking coincides more closely with GeBi<sub>2</sub>Te<sub>4</sub> and PbBi<sub>2</sub>Se<sub>4</sub>. In addition, Ge and Sb reciprocally occupy both the 3(*a*) and 6(*c*) sites. The Pb/Bi ratio is equal regardless of the sites in PbBi<sub>2</sub>Se<sub>4</sub>; on the other hand, the Ge/Sb ratio varies depending on the sites in the GeSb<sub>2</sub>Te<sub>4</sub> we analyzed.

As shown in Fig. 8, the atomic position *z* of each variable site is almost constant regardless of temperature, and the Ge/Sb ratio is also invariant. This means that in the structure of the stable phase the relative positions of atoms alter very little regardless of temperature changes, as did the structure of the metastable phase. Even when heated up to around the melting point, the structure did not change into metastable or other crystal phases. In Fig. 7, however, we can see an endothermic peak at about 890 K, corresponding to the transition from the solid to the liquid phase. This peak is not a single peak: it has a shoulder on the low temperature side. This might suggest that the stable phase first changes into another crystal, which could be the NaCl-type metastable structure, and then into the liquid. This is a future subject for study.



Here, if *A* is assumed to be one block, the whole structure can be described as a three-layer structure of *ABC* (see Fig. 9). *B* and *C* are obtained by shifting *A* in the  $[\bar{1}10]$  direction by  $\frac{1}{3}$  and  $\frac{2}{3}$ , respectively. We therefore conclude that the metastable phase transits to the stable phase as a result of vacancy diffusion. DSC measurements revealed the activation energy necessary for this phase transition by atomic diffusion to be approximately 4.0 eV.

As seen in Fig. 4, when the structure changes from the metastable phase to the stable phase, a discontinuity in volume is observed. In addition, the space group of the stable phase ( $R\bar{3}m$ ) is not a subgroup of the symmetry of the metastable phase ( $Fm\bar{3}m$ ).<sup>19</sup> This fact also proves that this structure transformation is a first-order phase transition.<sup>20</sup>

## V. CONCLUSIONS

The materials suitable for high-speed phase-change optical memories, GeTe-Sb<sub>2</sub>Te<sub>3</sub> and pseudobinary Au<sub>25</sub>Ge<sub>4</sub>Sn<sub>11</sub>Te<sub>60</sub> and Ag<sub>3.4</sub>In<sub>3.7</sub>Sb<sub>76.4</sub>Te<sub>16.5</sub> quadruple compounds, crystallize, as a result of instantaneous laser annealing, into cubic or slightly deformed cubic structures in which two or more elements tend to occupy one lattice site at random. This is because when an amorphous solid is given thermal energy by laser irradiation and then rapidly cooled, the atomic migration length is so short that it crystallizes into a

## C. Phase transition mechanism

We now compare the crystal structures of the metastable and stable phases. The NaCl type can be described in hexagonal notation as a six-layer structure (Fig. 9). The Ge/Sb layer in the metastable phase includes vacancies up to 25 at. %. It is logical to assume that the atomic diffusion of Ge and Sb towards the vacancies, as shown in Fig. 9, triggers the structural transformation from the former to the latter. Microscopically, the following three processes are assumed to take place during transformation. (i) As shown in Fig. 10(A), mainly Ge atoms in the II layer move to the vacancies (1) in the III layer. (ii) As shown in Fig. 10(B), Ge or Sb atoms in the I layer move to the vacancies (2) in the II layer. (iii) As shown in Fig. 10(C), Te atoms shift toward the row of point defects (a prismatic dislocation loop) in the I layer which is created by the above atomic movements. Due to these vacancy diffusions and shifts of atoms, the following stacking structure for the stable phase can be formed inside the dotted line in the figure:

spatially isotropic structure in which the constituent atoms randomly occupy lattice sites.<sup>7</sup> Laser-annealed GeSb<sub>2</sub>Te<sub>4</sub> crystallizes into a cubic NaCl-type structure in which Ge and Sb atoms randomly occupy the 4(*b*) site. This structure contains so many vacancies [up to 25 at. % for the 4(*b*) site] that the mean volume per single atom is greater than that in the stable phase.

The metastable phase retains its structure up to around 500 K. Above this temperature, however, Ge or Sb atoms pass through the Te layers to fill the vacancies, and the crystal structure transforms into a complicated cubic close-packed structure with a 21-layer period. Once changed into the stable phase, the structure remains stable over a wide temperature range of 90 K to around the melting point, with no transformation to the metastable phase observed. We have found, however, a shoulder on the low temperature side of the endothermic peak showing a transition from the solid to the liquid phase. This shoulder suggests the existence of an intermediate phase in the transition process. There are many kinds of compounds with low symmetry and complicated structures, such as GeBi<sub>2</sub>Te<sub>4</sub> and PbBi<sub>2</sub>Se<sub>4</sub>, mentioned above. It is likely that these compounds, including GeSb<sub>2</sub>Te<sub>4</sub>, transform via intermediate structures with random atomic arrangements or high symmetry from the solid phase to the amorphous/liquid phase, and vice versa.<sup>21,22</sup> We will proceed with studies to clarify the phase transition

mechanism between solid and amorphous/liquid by effectively utilizing this laser crystallization method.

### ACKNOWLEDGMENTS

These experiments were fully supported by the use of the BL02B2 line at SPring-8, the Japan Synchrotron Radiation

Research Institute. We express sincere thanks to K. Kato at the Japan Synchrotron Radiation Research Institute, to Dr. Y. Kubota at the Department of Environmental Sciences, Faculty of Science, Osaka Women's University, and to Dr. E. Nishibori, Assistant Professor M. Takata, and Professor M. Sakata at the Department of Applied Physics at Nagoya University for their kind advice on the experiment and analysis.

\*Fax: +81-6-6906-3407. Email address: matunaga@mtr.mei.co.jp

<sup>1</sup>N. Kh. Abrikosov and G. T. Danilova-Dobryakova, *Izv. Akad. Nauk SSSR, Neorg. Mater.* **1**, 204 (1965).

<sup>2</sup>I. I. Petrov, R. M. Imamov, and Z. G. Pinsker, *Sov. Phys. Crystallogr.* **13**, 339 (1968).

<sup>3</sup>K. A. Agaev and A. G. Talybov, *Sov. Phys. Crystallogr.* **11**, 400 (1966).

<sup>4</sup>J. Goldak, C. S. Barrett, D. Innes, and W. Youdelis, *J. Chem. Phys.* **44**, 3323 (1966).

<sup>5</sup>R. W. G. Wyckoff, *Crystal Structures* (Krieger, Malabar, 1986), Vol. 2.

<sup>6</sup>N. Yamada, Ph.D. thesis, Kyoto University Doctoral Dissertation, 2000 (in Japanese).

<sup>7</sup>T. Matsunaga and N. Yamada, *Jpn. J. Appl. Phys.* **41**, 1674 (2002).

<sup>8</sup>T. Matsunaga, Y. Umetani, and N. Yamada, *Phys. Rev. B* **64**, 184116 (2001).

<sup>9</sup>N. Yamada and T. Matsunaga, *J. Appl. Phys.* **88**, 7020 (2000).

<sup>10</sup>E. Nishibori, M. Takata, K. Kato, M. Sakata, Y. Kubota, S. Aoyagi, Y. Kuroiwa, M. Yamakata, and N. Ikeda, *Nucl. Instrum. Methods Phys. Res. A* **467-468**, 1045 (2001).

<sup>11</sup>H. M. Rietveld, *J. Appl. Crystallogr.* **2**, 65 (1969).

<sup>12</sup>F. Izumi and T. Ikeda, *Meas. Sci. Technol.* **321-324**, 198 (2000).

<sup>13</sup>*International Tables for Crystallography*, edited by T. Hahn (Kluwer, Dordrecht, 1995), Vol. A.

<sup>14</sup>A. J. C. Wilson, *X-Ray Optics* (Methuen, London, 1949).

<sup>15</sup>K. A. Agaev and S. A. Semiletov, *Sov. Phys. Crystallogr.* **10**, 86 (1965).

<sup>16</sup>K. A. Agaev and S. A. Semiletov, *Sov. Phys. Crystallogr.* **13**, 201 (1968).

<sup>17</sup>N. Yamada, E. Ohno, K. Nishiuchi, and N. Akahira, *J. Appl. Phys.* **69**, 2849 (1991).

<sup>18</sup>*Handbook of Thermal Analysis*, edited by T. Hatakeyama and Zhenhai Liu (Wiley, Chichester, 1998).

<sup>19</sup>B. K. Vainshtein, V. M. Fridkin, and V. L. Indenbom, *Structure of Crystals* (Springer-Verlag, Berlin, 1995).

<sup>20</sup>L. D. Landau, A. I. Akhiezer, and E. M. Lifshits, *General Physics* (Pergamon, Oxford, 1967).

<sup>21</sup>W. Ostwald, *Z. Phys. Chem., Stoechiom. Verwandtschaftsl.* **22**, 289 (1897).

<sup>22</sup>K. N. Ishihara and P. H. Shingu, *Mater. Sci. Eng.* **63**, 251 (1984).